AIP Journal of Applied Physics

Dependence of optimized annealing temperature for tetragonal phase formation on the Si concentration of atomic-layer-deposited Hf-silicate film

Hyo Kyeom Kim, Hyung-Suk Jung, Jae Hyuck Jang, Jinho Park, Tae Joo Park et al.

Citation: J. Appl. Phys. **110**, 114107 (2011); doi: 10.1063/1.3665411
View online: http://dx.doi.org/10.1063/1.3665411
View Table of Contents: http://jap.aip.org/resource/1/JAPIAU/v110/i11
Published by the American Institute of Physics.

Additional information on J. Appl. Phys.

Journal Homepage: http://jap.aip.org/
Journal Information: http://jap.aip.org/about/about_the_journal
Top downloads: http://jap.aip.org/features/most_downloaded
Information for Authors: http://jap.aip.org/authors

ADVERTISEMENT

Downloaded 18 Apr 2013 to 143.248.118.125. This article is copyrighted as indicated in the abstract. Reuse of AIP content is subject to the terms at: http://jap.aip.org/about/rights_and_permissions

Dependence of optimized annealing temperature for tetragonal phase formation on the Si concentration of atomic-layer-deposited Hf-silicate film

Hyo Kyeom Kim,[1] Hyung-Suk Jung,[2] Jae Hyuck Jang,[2] Jinho Park,[2] Tae Joo Park,[3] Seok-Hee Lee,[4] and Cheol Seong Hwang[2,a)]

[1]*Department of Nano Science and Technology, Graduate School of Convergence Science and Technology, Seoul National University, Suwon 443-270, South Korea*
[2]*WCU Hybrid Materials Program, Department of Materials Science and Engineering and Inter-University Semiconductor Research Center, Seoul National University, Seoul 151-744, South Korea*
[3]*Department of Materials Engineering, Hanyang University, Ansan, 426-791, South Korea*
[4]*Department of Electrical Engineering, Korea Advanced Institute of Science and Technology, Daejeon, 305-701, South Korea*

(Received 8 September 2011; accepted 29 October 2011; published online 2 December 2011)

This study examined the relation between the permittivity and microstructures of atomic layer deposited $Hf_{1-x}Si_xO_2$ (HfSiO) thin films with different Si concentrations as a function of post-deposition annealing (PDA) temperature. The PDA at high temperature results in the separation of crystallized HfO_2 phase from the much higher Si-containing amorphous-like matrix. Tetragonal phase HfO_2 formation with higher permittivity than the monoclinic HfO_2 phase is induced with an appropriate Si concentration in the film (∼10–20%). In the crystallized HfSiO film, the Si concentration in the phase-separated HfO_2 (mainly consisting of HfO_2) could be controlled by PDA temperature, which determines the degree of phase separation. The increased PDA temperature reduces the Si concentration in the phase-separated HfO_2, which induced monoclinic phase formation. Therefore, the PDA temperature for maximized permittivity of the crystallized HfSiO films (maximized tetragonal phase portion in the film) depends on the Si concentration of the HfSiO film in the as-deposited state. © *2011 American Institute of Physics*. [doi:10.1063/1.3665411]

I. INTRODUCTION

One of the key methods to enable transistor channel length scaling in complementary metal-oxide-semiconductor field effect transistors (CMOSFETs) is to scale the gate dielectrics. However, with this method, scaling slows down at the 90 nm node as SiO_2 runs out of atoms and further scaling of the gate-leakage current is limited.[1] To decrease the gate leakage in highly scaled transistors, Hf and Zr-based high-k gate dielectrics have been considered to be the most promising candidates to replace SiO_2 gate dielectrics.[2–4] Hf-based high-k gate dielectrics have already been employed in the current technology node.[5] $Hf_{1-x}Si_xO_2$ (HfSiO) gate dielectrics as an alternative to HfO_2 have advantages such as increased crystallization temperature,[6] reduced growth of the interfacial oxide layer at the silicon/high-k interface,[7] and higher bandgap.[8]

Recently, two basic approaches were introduced for the integration of gate stacks using high-k gate dielectrics and a metal gate electrode: A gate-first approach[9] and a gate-last approach.[10] In the gate-first approach, the high-k gate dielectrics need to have high thermal stability, because of the formation of the gate stack before activation annealing of the source and drain, as in a conventional CMOSFET process. Therefore, Hf-silicate film would be a suitable candidate for the gate-first process, because of its high thermal stability as well as its process maturation. In gate-last approach, the thermal stability of the gate dielectric is not crucial.

The incorporated Si in HfO_2 films does not only increase the crystallization temperature but also changes the crystalline phase.[11–13] A certain concentration of Si in HfSiO film induced the crystalline phase transformation of the film from monoclinic to tetragonal, over which the sacrifice of the permittivity was observed.[14] The tetragonal phase has a higher permittivity than that of monoclinic phase, so that achieving the tetragonal phase is desirable. Optimization of the post-deposition annealing (PDA) temperature for crystallization of the film is crucial, as much as that of Si concentration in the film for tetragonal phase formation, because high-temperature annealing induces Si diffusion from a substrate into the film and an interfacial layer growth, which would deteriorate the overall permittivity of the film.[15]

Therefore, in this study, the PDA temperature for phase transformation of atomic layer deposited HfSiO film with various Si concentrations was systematically examined and optimized. Although there have been many reports on the structural and electrical changes in the HfSiO film with the PDA process, the detailed study on the structural evolution of the film and accompanying dielectric properties depending on the Si concentration has not been reported. In addition, the analysis data for the relevant thickness range ($\ll$ 10 nm) is quite rare. In this study, therefore, the changes in the microstructure of HfSiO film with various annealing temperatures and Si concentrations were traced by high-resolution transmission electron microscopy (HRTEM), and the electrical properties of the various films were also examined.

a)Electronic mail: cheolsh@snu.ac.kr.

 © 2011 American Institute of Physics

Downloaded 18 Apr 2013 to 143.248.118.125. This article is copyrighted as indicated in the abstract. Reuse of AIP content is subject to the terms at: http://jap.aip.org/about/rights_and_permissions

II. EXPERIMENTAL PROCEDURES

HfSiO films were deposited on HF cleaned p-type Si (100) substrates by atomic layer deposition (ALD) at a wafer temperature of 270 °C, using Tetrakis[EthylMethylAmino]-Hafnium ($Hf[N(CH_3)(C_2H_5)]_4$) and Tris(DiMethylAmino) Silane ($SiH[N(CH_3)_2]_3$) as precursors and ozone gas (concentration of 170 gm^{-3}) as the oxygen source. The Si/(Hf + Si) concentration in the HfSiO film was controlled from 14% to 81%. The ALD grown HfO_2 and SiO_2 films were also included as references to compare their properties with HfSiO films. The HfSiO films were deposited by the appropriate control of the cycle ratio of HfO_2 and SiO_2 film growth processes. (See Fig. 1(a)) The precursor pulse/purge/ozone pulse/purge times for the HfO_2 and SiO_2 films were 3/20/3/10 s and 3/15/3/10 s, respectively, which were identified as the well-saturated ALD conditions. The physical thicknesses of various HfSiO films measured by ellipsometry were ~10 nm and ~3–8 nm for physical and electrical analysis, respectively. PDA was performed by rapid thermal process (RTP) at temperatures ranging from 400 to 1000 °C under N_2 atmosphere for 30 s. Any notable decrease in the film thickness was not observed after PDA for both HfO_2 and HfSiO film, confirmed by the ellipsometry and HRTEM,[16] due to the low impurity concentration, confirmed by Auger electron spectroscopy depth profiles (not shown here), and relatively high density of as-deposited films. The theoretical volumetric shrinkage caused by the transformation of HfO_2 from monoclinic to tetragonal phase is only 3.6%.[14] In addition, only part of the film shows the phase transition during the PDA, so that the overall volume change by the phase transition must be negligible ($<\sim 2\%$). Therefore, it is considered that the densification of the films can hardly affect the permittivity. A circular shape 80-nm-thick Pt top electrode with a 300 μm diameter was deposited though metal shadow mask by dc magnetron sputtering to fabricate metal-insulator-semiconductor (MIS) capacitors for electrical measurements. Capacitance-voltage (C-V) and gate-leakage current density-voltage (J_g-V) characteristics were examined using a Hewlett-Packard 4194 A Impedance/Gain-Phase analyzer and a Hewlett-Packard 4140B pA meter/dc voltage source, respectively. The capacitance equivalent thickness (CET) was calculated from the accumulation capacitance in the measure C-V curves at a frequency of 100 kHz with a voltage sweep range from −2.5 to + 2.5 V. The chemical bonding states in the HfSiO films with various Si/(Hf + Si) ratios were examined by x-ray photoelectron spectroscopy (XPS; AXIS-His). The crystallinity of the HfSiO films was estimated by a glancing angle x-ray diffraction (GAXRD, PANalytical X'Pert PRO MPD), and the microstructure of the films was analyzed using a HRTEM (Tecnai F20, field-emission, 200 kV), Fast Fourier Transformation (FFT), and the electron energy loss spectroscopy (EELS; GIF Tridiem 863).

III. RESULTS AND DISCUSSION

Figure 1(a) shows the ALD super-cycle schematic for HfSiO film, which consists of a HfO_2 sub-cycle and a SiO_2 sub-cycle. The composition of Si/(Hf + Si) in HfSiO films was controlled using the number of HfO_2 and SiO_2 sub-cycles in a super-cycle. The growth rates of HfO_2 and SiO_2 film were 0.12 and 0.072 nm per cycle, respectively. The sub-cycle ratio of the SiO_2 sub-cycle to the HfO_2 sub-cycle was controlled from 3:1 to 1:9, which corresponds to the Si/(Hf + Si) feeding ratio from 0.75 to 0.1. The growth rate per a super-cycle of HfSiO film is comparable with the summation of component sub-cycle growth rate, which is 0.12 × HfO_2 sub-cycle number + 0.072 × SiO_2 sub-cycle number. For examples, the growth rate per a super-cycle of HfSiO films with Si:Hf feeding ratio of 0.75 (3:1), 0.5 (1:1), and 0.125 (1:7) was 0.35 nm, 0.2 nm, and 0.91 nm, respectively. This means the growth behavior of HfO_2 and SiO_2 sub-cycles are maintained in the HfSiO super-cycles. In other words, the growth of Hf-O layer on Si-O terminating surface is almost identical to that on the Hf-O surface itself, and growth of Si-O layer on Hf-O terminating surface is almost identical to that on the Si-O surface itself. Figure 1(b) shows that the Si/(Hf + Si) atomic ratios in HfSiO films have a linear relation with the Si/(Hf + Si) feeding ratio controlled by the sub-cycle ratio. The Si/(Hf + Si) atomic ratios were extracted from the area ratio of XPS Hf 4*f* peak and Si 2*p* peak. The Si atomic concentration of HfSiO films with the Si/(Hf + Si) feeding ratio of 0.75 (3:1), 0.5 (1:1), 0.25 (1:3), and 0.125 (1:7) is 81%, 57%, 33%, and 16%, respectively.

Figures 2(a) and 2(b) shows Hf 4*f* and Si 2*p* core levels XPS spectra, respectively, for as-deposited HfO_2, SiO_2, and HfSiO films with various Si concentrations. The binding energy of all peaks has been calibrated by centering the carbon 1*s* peak at 284.5 eV. In Fig. 2(a), HfO_2 (top black line) shows a sharp doublet according to spin-orbital splitting into

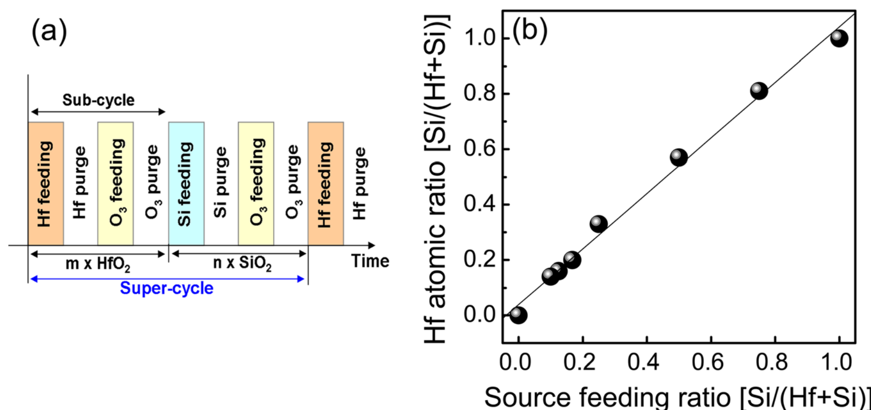

FIG. 1. (Color online) (a) Schematic diagram of ALD super-cycle of HfSiO film consisting of HfO_2 and SiO_2 sub-cycle and (b) the correlation graph between the source feeding ratio, calculated by sub-cycle feeding number, and the atomic ratio, estimated from XPS peak area ratio of Hf 4*f* and Si 2*p*.

Downloaded 18 Apr 2013 to 143.248.118.125. This article is copyrighted as indicated in the abstract. Reuse of AIP content is subject to the terms at: http://jap.aip.org/about/rights_and_permissions

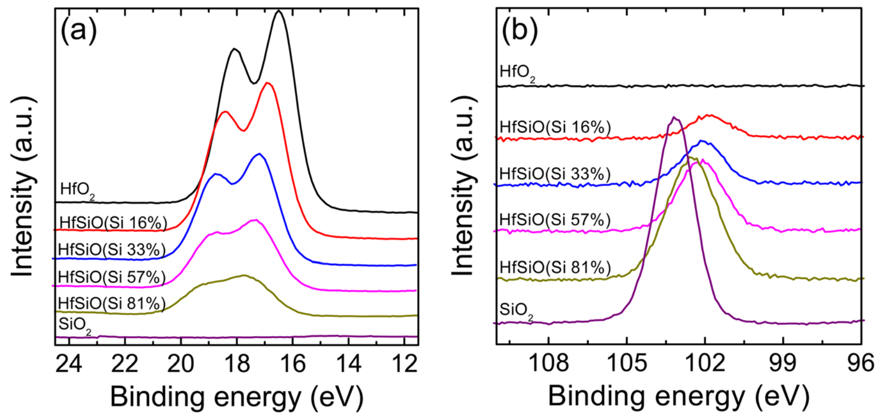

FIG. 2. (Color online) (a) Hf 4*f* and (b) Si 2*p* core level XPS spectra for HfSiO films with Si:Hf ratio of 1:7 (Si 16%) to 3:1 (Si 81%), including ALD grown HfO_2 and SiO_2.

Hf $4f_{5/2}$ and Hf $4f_{7/2}$ peaks with binding energies of 18.2 eV and 16.6 eV, respectively, which is consistent with the data reported previously.[17] In general, as the Si concentration in HfSiO increases, the Hf 4*f* peak position gradually shifts to higher binding energy direction with the distortion of the peak shape. This is because the increased Si-O bonds in the film affect the Hf-O bonding characteristics.[18]

Figure 2(b) shows the Si 2*p* core level XPS spectra of the same samples shown in Fig. 2(a). The binding energy of the Si 2*p* peak of HfSiO increased with increasing Si concentrations, from 101.7 eV (HfSiO with a Si concentration of 16%) to 103.2 eV (ALD grown SiO_2), which is consistent with the previous report that Si-O bonding energy in SiO_2 shifts to lower energy because of the change of Si's second nearest neighbor from Si to Hf.[18,19]

Figure 3(a) shows the variation of permittivity of as-deposited HfO_2, SiO_2, and HfSiO films as a function of the Si concentration. The permittivity was extracted by dividing 3.9 by the slope of the CET versus thickness plot as shown in Fig. 3(c), which excludes the influence of the interfacial layer. The Si incorporation into the film led to lower permittivity.

However, the change in the permittivity of HfSiO films after PDA depends on the Si concentration in the film, as shown in Fig. 3(b). Here, the permittivity was also calculated from the slope of the CET versus thickness curves, one example of which is also included in Fig. 3(c) for the HfSiO films with a Si concentration of 16%. The as-deposited HfO_2 film in this thickness range was amorphous and has a bulk permittivity of 17.5. After the PDA at 700 and 800 °C, the HfO_2 film crystallized into a monoclinic phase as shown in Fig. 3(d), which was evidenced by the inset FFT pattern. The permittivity was slightly decreased to 14 due to the Si diffusion from a substrate into the film during PDA. It must be noted that the Si-diffusion from the substrate does not induce the phase transformation of HfO_2 phase from monoclinic to tetragonal. This suggests that the diffused Si atoms from the substrate do not diffused into the crystallizing grains of HfO_2. However, the situation is quite different when the crystallization proceeds from the HfSiO film as shown below.

In the case of HfSiO with a Si concentration of 16%, although the permittivity of the as-deposited film was quite low (~11), the permittivity of the film increased two times compared to that of as-deposited film after PDA at 800 °C (~21) as shown in Fig. 3(b). This is attributed to the tetragonal phase formation in the film by PDA at 800 °C. It is believed that the presence of SiO_2 component in the as-deposited film induced the crystallization of the HfSiO film with the tetragonal phase. Interestingly, the permittivity of HfSiO film with a Si concentration of 16% decreased after PDA above 900 °C. This could be induced by the transformation from tetragonal to monoclinic of the separated HfO_2 phase. This was confirmed by HRTEM result in Fig. 4 that shows the typical HRTEM micrographs of HfSiO film with a Si concentration of 16% after PDA at (a) 800 °C and (b) 1000 °C. Although it is not clearly resolved in those figures, the crystallized films show segregation of phases into several crystalline phases, and each phase was identified using the FFT technique. The change in the phase ratio in the film as a function of PDA temperature was summarized in Fig. 4(c), where the phase information of the film was randomly

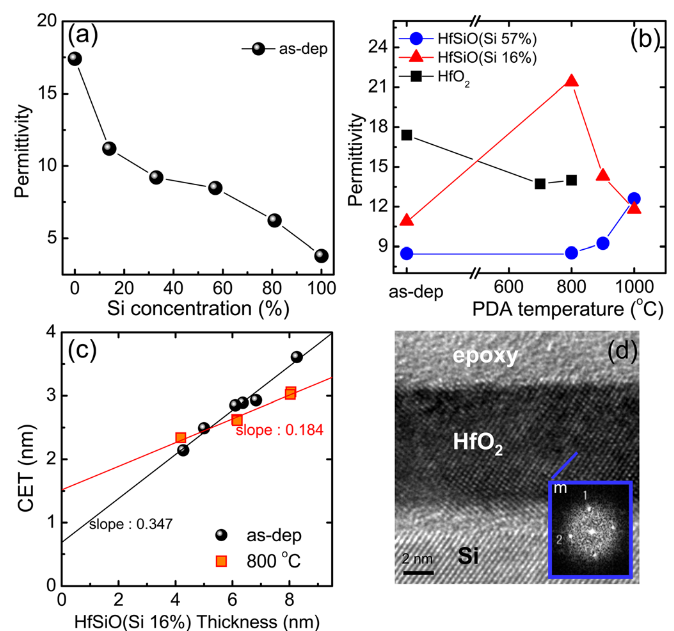

FIG. 3. (Color online) (a) The permittivity of as-deposited HfSiO films as a function of Si concentrations and (b) the permittivity changing as a function of PDA temperatures for HfO_2 and HfSiO films with Hf:Si ratio of 1:1 (Si 57%) and 1:7 (Si 16%). For the evaluation of permittivity, (c) the inverse slope of the CET vs physical thickness for HfSiO film with Si 16% before and after PDA (800 °C), and (d) TEM image and FFT pattern of HfO_2 after PDA (700 °C).

Downloaded 18 Apr 2013 to 143.248.118.125. This article is copyrighted as indicated in the abstract. Reuse of AIP content is subject to the terms at: http://jap.aip.org/about/rights_and_permissions

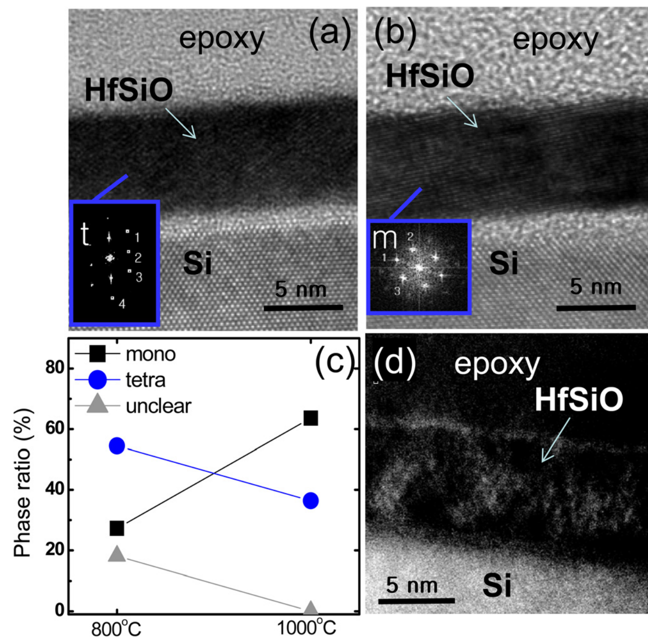

FIG. 4. (Color online) TEM micrographs and FFT patterns of about 7-nm-thick HfSiO films with Si concentration of 16% after PDA at (a) 800 °C and (b) 1000 °C for 30 s in N_2 atmosphere and (c) the phase ratio of both films analyzed from randomly selected 30 points by FFT and (d) EELS mapping image of Si of the film after 1000 °C for 30 s in N_2 atmosphere.

collected from more than 30 points from the HRTEM images. Here, the "unclear" region corresponds to the crystallized part but unequivocal identification of phase is not possible perhaps due to the overlapping lattice images. After the PDA at temperatures higher than 800 °C, the films were almost fully crystallized, but the distribution of the phase varies with the PDA temperature. While the tetragonal phase ratio in the film decreased, the monoclinic phase ratio in the film increased with an increased PDA temperature. This can be understood from the following. The metastable amorphous HfSiO film crystallizes with separated phases of Hf-rich and Si-rich regions, which must be more amorphous-like structure, during the PDA. It is believed that the tetragonal phase formation, which is induced with the help of a certain amount of Si incorporated in the film (~10–20%),[12] was disturbed by the deficiency of Si in the film because of the severe phase separation of the film into SiO_2 (mainly consisted of SiO_2) and HfO_2 (mainly consisted of HfO_2) after PDA above 900 °C. The phase separation of the film after PDA at 1000 °C is rarely observed in the HRTEM image of Fig. 4(b), due to the overlap of crystalline image with amorphous-like image. However, the EELS mapping image of the Si of the HfSiO film after PDA at 1000 °C in Fig. 4(d) confirmed that the separated SiO_2 phase segregated at the film surface and partially in the film, which is indicated by white region in the figure.[11] The enhanced Si diffusion from the substrate into the film also contributed to the decreased permittivity of the film.

In the case of HfSiO film with the Si concentration of 57%, the permittivity of the film remained at the low value (~8) up to the PDA temperature of 800 °C, due to the retained amorphous structure [Fig. 5(a)], but increased at the PDA temperature of 1000 °C. It is notable that the permittivity of the film with such a high Si concentration (57%) is comparable to that of the film with the lower Si concentration (16%) after the PDA at 1000 °C. This can be understood from the composition of formed phases at that temperature as shown in Fig. 5. The XRD patterns of the HfSiO film with Si concentration of ~57% before and after PDA at various temperatures in Fig. 5(a) show that the crystalline temperature of the film reached to 1000 °C (although the nano-crystalline structure might be formed below 1000 °C). The HRTEM micrograph of the film with FFT images [Fig. 5(b)] and the phase ratio in the film [Fig. 5(c)] show that the portion of tetragonal phase in the HfSiO film with Si concentration of 57% after PDA at 1000 °C (~50%) is higher than that of the film with Si concentration of 16% (~35%). Figure 5(b) clearly shows the separated crystalline phases with remaining amorphous parts due to the higher Si concentration. This is due to that the remaining Si concentration in the separated (mostly) HfO_2 phase is higher compared to the other case because of the originally higher Si concentration. Then, this higher Si concentration in the HfO_2 phase retains the tetragonal phase more efficiently. PDA at an even higher

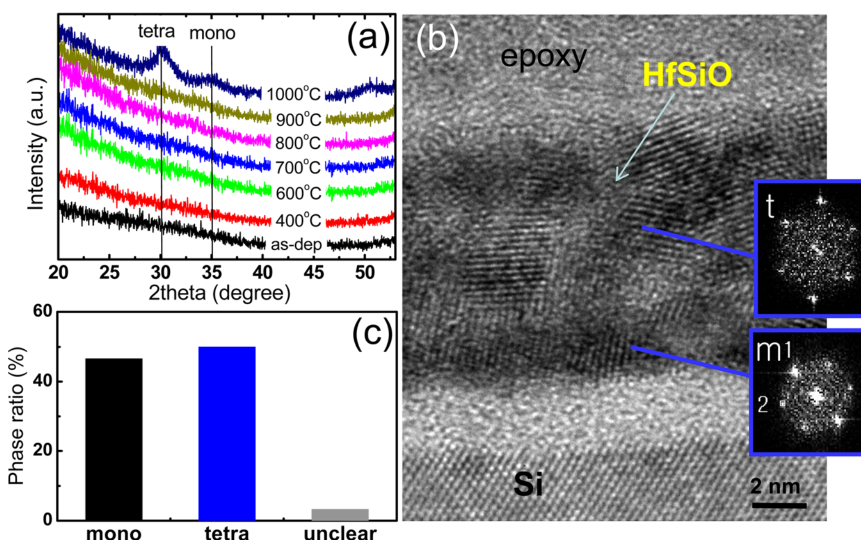

FIG. 5. (Color online) (a) XRD patterns of HfSiO films with Si concentration of 57% after PDA from 400 °C to 1000 °C for 30 s under N_2 atmosphere, (b) TEM micrographs and (inset) FFT patterns, and (c) the phase ratio of the film after PDA 1000 °C for 30 s.

Downloaded 18 Apr 2013 to 143.248.118.125. This article is copyrighted as indicated in the abstract. Reuse of AIP content is subject to the terms at: http://jap.aip.org/about/rights_and_permissions

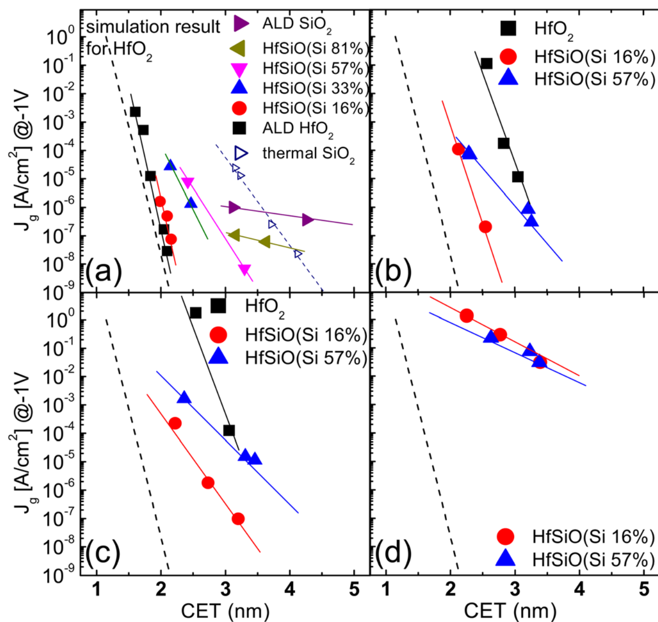

FIG. 6. (Color online) Plot of CET vs J_g for (a) as-deposited HfO_2 and HfSiO films with various Si concentrations, and annealed HfO_2 and HfSiO films with a Si concentration of 16 and 57% at (b) 800 °C, (c) 900 °C, and (d) 1000 °C 30 s (simulation result for HfO_2 is indicated by a dashed line).

temperature, over 1000 °C, of the film might induce the decrease in the permittivity, because the further reduction of Si concentration in the separated HfO_2 phase (further phase separation) would enhance more monoclinic phase formation. However, this cannot be confirmed experimentally owing to the limited temperature condition for the RTP system (max. 1000 °C) used in this study.

Figure 6 shows the plot of J_g versus CET of the HfO_2 and HfSiO films with various Si concentrations before and after PDA at 800, 900, and 1000 °C. Simulation result for HfO_2 film indicated by a dash line and experimental result for pure SiO_2 film were also included for comparison.[20] The insulating property of the as-deposited films degrades with increasing Si concentration because of the low permittivity of SiO_2, as shown in Fig. 6(a). However, the insulating property of HfO_2 film drastically degrades after PDA at temperatures higher than 800 °C, which is worse than even that of HfSiO film with a Si concentration of 57% [Fig. 6(b)]. In contrast, HfSiO film with a Si concentration of 16% keeps the promising insulating property after PDA up to 900 °C [Fig. 6(c)]. HfSiO film with a Si concentration of 57% also has promising thermal stability, but the CET is generally large because of a high Si concentration. After PDA at 1000 °C, the result for HfO_2 film is hard to obtain because the J_g of HfO_2 film is too large to achieve the stable C-V curves. Both HfSiO films with a Si concentration of 16 and 57% also degrade severely, to a similar level, after PDA at 1000 °C [Fig. 6(d)]. The insulating property of HfSiO film with a Si concentration of 16% seems to degrade more abruptly with increasing PDA temperature, which is attributed to the decreased permittivity of the film after PDA over 800 °C. Nevertheless, it should be noted that HfSiO film with a Si concentration of 16% showed superior electrical performance up to 900 °C.

IV. CONCLUSION

The relation between the permittivity and the micro structures of atomic layer deposited HfSiO films with various Si concentrations as a function of PDA temperature was systematically examined using MIS capacitor and HRTEM analysis. The permittivity of the crystallized HfSiO films with a Si concentration of ∼16% abruptly increased after PDA at 800 °C, because of tetragonal phase formation with the help of an appropriate amount of Si in the film. However, it decreased after PDA at 1000 °C, because the crystallization proceeds with higher proportion of monoclinic HfO_2 phase due to more severe segregation of Si into the SiO_2 phase. In contrast, the permittivity of HfSiO films with a Si concentration of ∼57% increased considerably after PDA at 1000 °C, because an appropriate Si concentration remained in the separated HfO_2 to form the tetragonal phase due to the initially high Si concentration. The electrical measurement showed that an optimized Si concentration (∼16%) in the HfSiO film maintained promising electrical properties up to 900 °C. However, the PDA at 1000 °C degraded the electrical performance severely irrespective of the Si concentration.

ACKNOWLEDGMENTS

The authors acknowledge support by the system IC 2010 project of the Korean Government through Hynix Company, and the Convergent Research Center program (Grant No. 2011K000610), through the National Research Foundation of Korea funded by the Ministry of Education, Science, and Technology.

[1]S. Thompson, N. Anand, M. Armstrong, C. Auth, B. Arcot, M. Alavi, P. Bai, J. Bielefeld, R. Bigwood, J. Brandenburg, M. Buehler, S. Cea, V. Chikarmane, C. Choi, R. Frankovic, T. Ghani, G. Glass, W. Han, T. Hoffmann, M. Hussein, P. Jacob, A. Jain, C. Jan, S. Joshi, C. Kenyon, J. Klaus, S. Klopcic, J. Luce, Z. Ma, B. Mcintyre, K. Mistry, A. Murthy, P. Nguyen, H. Pearson, T. Sandford, R. Schweinfurth, R. Shaheed, S. Sivakumar, M. Taylor, B. Tufts, C. Wallace, P. Wang, C. Weber, and M. Bohr, Tech. Dig. – Int. Electron Devices Meet. 2002, p. 61.
[2]G. D. Wilk, R. M. Wallace, and J. M. Anthony, J. Appl. Phys. **89**, 5243 (2001).
[3]J. Robertson, Rep. Prog., Phys. **69**, 327 (2006).
[4]K. Kukli, T. Pilivi, M. Ritala, T. Sajavaara, J. Lu, and M. Leskela, Thin Solid Films **491**, 328 (2005).
[5]K. Mistry, C. Allen, C. Auth, B. Beattie, D. Bergstrom, M. Bost, M. Brazier, M. Buehler, A. Cappellani, R. Chau, C.-H. Choi, G. Ding, K. Fischer, T. Ghani, R. Grover, W. Han, D. Hanken, M. Hattendorf, J. He, J. Hicks, R. Huessner, D. Ingerly, P. Jain, R. James, L. Jong, S. Joshi, C. Kenyon, K. Kuhn, K. Lee, H. Liu, J. Maiz, B. McIntyre, P. Moon, J. Neirynck, S. Pae, C. Parker, D. Parsons, C. Prasad, L. Pipes, M. Prince, P. Rarade, T. Reynolds, J. Sandford, L. Shifren, J. Sebastian, J. Seiple, D. Simon, S. Sivakumar, P. Smith, C. Thomas, T. Troeger, P. Vandervoorn, S. Williams, and K. Zawadzki, Tech. Dig. - Int. Electron Devices Meet. 2007, p. 247.
[6]A.L.P. Rotondaro, M. R. Visokay, J. J. Chambers, A. Shanware, R. Khamankar, H. Bu, R. T. Laaksonen, L. Tsung, M. Douglas, R. Kuan, M. J. Bevan, T. Grider, J. McPherson, and L. Colombo, Dig. Tech. Pap. - Symp. VLSI Technol. 2002, p. 148.
[7]M. Lemberger, A. Paskaleva, S. Zürcher, A. J. Bauer, L. Frey, and H. Ryssel, Microelectron. Reliab. **45**, 819 (2005).
[8]J. Robertson, J. Vac. Sci. Technol. B. **18**, 1785 (2000).
[9]M. Chudzik, B. Doris, R. Mo, J. Sleight, E. Cartier, C. Dewan, D. Park, H. Bu, W. Natzle, W. Yan, C. Ouyang, K. Henson, D. Boyd, S. Callegari, R. Carter, D. Casarotto, M. Gribelyuk, M. Hargrove, W. He, Y. Kim, B. Linder, N. Moumen, V. K. Paruchuri, J. Stathis, M. Steen, A. Vayshenker, X. Wang,

Downloaded 18 Apr 2013 to 143.248.118.125. This article is copyrighted as indicated in the abstract. Reuse of AIP content is subject to the terms at: http://jap.aip.org/about/rights_and_permissions

S. Zafar, T. Ando, R. Iijima, M. Takayanagi, V. Narayanan, R. Wise, Y. Zhang, R. Divakaruni, M. Khare, and T. C. Chen, Dig. Tech. Pap. - Symp. VLSI Technol., 2007, p. 194.
[10] P. Packan, S. Akbar, M. Armstrong, D. Bergstrom, M. Brazier, H. Deshpande, K. Dev, G. Ding, T. Ghani, O. Golonzka, W. Han, J. He, R. Heussner, R. James, J. Jopling, C. Kenyon, S-H. Lee, M. Liu, S. Lodha, B. Mattis, A. Murthy, L. Neiberg, J. Neirynck, S. Pae, C. Parker, L. Pipes, J. Sebastian, J. Seiple, B. Sell, A. Sharma, S. Sivakumar, B. Song, A. St. Amour, K. Tone, T. Troeger, C. Weber, K. Zhang, Y. Luo, and S. Natarajan, Tech. Dig. - Int. Electron Devices Meet. 2009, p. 659.
[11] T. J. Park, J. H. Kim, J. H. Jang, K. D. Na, C. S. Hwang, and J. H. Yoo, Electrochem. Sol. State. Lett. **11**, 121 (2008).
[12] K. Tomida and A. Toriumi, Appl. Phys. Lett. **89**, 142902 (2005).
[13] D. A. Neumayer and E. Cartier, J. Appl. Phys. **90**, 1801 (2001).
[14] C. K. Lee, E. Cho, H. -S. Lee, C. S. Hwang, and S. Han, Phys. Rev. B **78**, 012102 (2008).
[15] T. J. Park, J. H. Kim, J. H. Jang, C. -K. Lee, K. D. Na, S. Y. Lee, H. -S. Jung, M. Kim, S. Han, and C. S. Hwang, Chem. Mater. **22**, 4175 (2010).
[16] H.-S. Jung, J. H. Jang, D.-Y. Cho, S.-H. Jeon, H. K. Kim, S. Y. Lee, and C. S. Hwang, Electrochem. Sol. State. Lett. **14**, 17 (2011).
[17] D. Triyoso, R. Liu, D. Roan, M. Ramon, N. V. Edwards, R. Gregory, D. Werho, J. Kulik, G. Tam, E. Irwin, X.-D. Wang, L. B. La, C. Hobbs, R. Garcia, J. Baker, B. E. White, and P. Tobina, J. Electrochem. Soc. **151**, F220 (2004).
[18] K. Chang, K. Shanmugasundaram, J. Shallenberger, and J. Ruzyllo, Thin Solid Films **515**, 3802 (2007).
[19] H. Jin, S. K. Oh, H. J. Kang, and M. -H. Cho, Appl. Phys. Lett. **89**, 122901 (2006).
[20] Y.-C. Yeo, T.-J. King, and C. Hu, Appl. Phys. Lett. **81**, 2091 (2002).

Downloaded 18 Apr 2013 to 143.248.118.125. This article is copyrighted as indicated in the abstract. Reuse of AIP content is subject to the terms at: http://jap.aip.org/about/rights_and_permissions